Theoretical Modelling of An End Face Reflection based Tapered Fiber Optic SPR Sensor with Different Probe Designs

Rajneesh. K. Verma
Department of Physics
Central University of Rajastha
Bander Sindri, Ajmer, India

***Abstract* - The theoretical modelling of a SPR based tapered fiber optic sensor is presented with the end face as a reflecting surface. The performance of the sensor is evaluated in terms of its sensitivity and detection accuracy with taper ratio. Apart from this, the effect of various taper profiles on to the sensitivity of the sensor is also studied. It has been found in the present study that the end face reflection technique reduces the size of the sensor probe and makes it miniaturized. The maximum sensitivity of the exponential taper profile makes it an optimum taper profile among the three profiles named linear, parabolic and exponential.**

Keywords* - *Surface Plasmons, Fiber Optics, Tapered Fiber, Plasmons

I. INTRODUCTION

Surface plasmons resonance (SPR) is a very promising tool for the sensing of various biochemical and gaseus sensing [1-12]. A vast number of researchers are engaged in this upcoming area to explore various possibilities in terms of making fiber optic probes for the continuous monitoring of changes occurring in biochemical, chemical and gasesus media [12-27]. Recently many theoretical models have been proposed for the better sensing mechanisms such as localized surface plasmon based fiber optic sensors [3], use of conducting metal oxides is also an important study [10]-[14]. In the last year people have fabricated and characterized the fiber optic sensing probes for pH sensing [10] and H2S gas sensing [11]. Sensing of Phenolic compounds and Ammonia gas sensing has also been proposed [12]-[13]. Fiber optic grating is also being used in conjunction with spr to make a miniaturized fiber optic probe for sensing the refractive indecies [14]-[15]. Most recently people are also proposing certain models on optical waveguides which involves artificially structured materials such metamaterials as a SPR active material [16]. In this study a theoretical model has been proposed which involes the multimoded tapered optical fibers. Contrary to the conventional fiber optic probes, in the present probe the one of the end face is coated with a silver paste to make it reflecting. This probe proposed in the model will be miniaturized as well as it will work as a point sensor as its one end can be dipped directly in to the medium to which we are going to sense. The performance parameters such as sensitivity have also been evaluated in terms of the taper ratio. Effect of various taper profiles such as linear, parabolic and exponential linear has also been studied and a comparative analysis has also been provided in terms of the best taper profile for the sensitivity among the rest of the two.

II. THEORETICAL MODEL

The theoretical model is based on the principle of attenuated total reflection (ATR) with Kretschmann configuration. The plastic cladding from the middle portion of a step index multimode fiber is removed and the unclad portion is tapered. The unclad tapered region is then cut from the point where the waist diameter is minimum. The unclad tapered fiber region is then coated with a thin gold layer, which is further surrounded by sensing medium (Fig. 1).

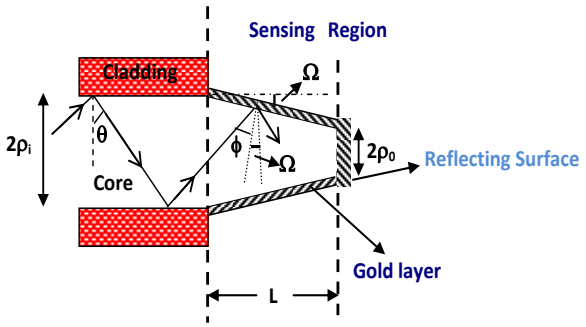

Figure 1: A typical SPR based fiber optic sensor with tapered probe.

Different taper profiles can be generated during fabrication using "Flame Brush" technique as suggested by Birks and Li [23]-[24]. The method uses a point like heat source (a gas burner) which heats only a small section of the fiber at a time. This burner is made to travel at constant speed in an oscillatory manner along the distance of the fiber (to be tapered) so that in each cycle of oscillation every element of the fiber is heated identically. If the speed of the burner is large compared to the tapered elongation speed then a time averaged hot – zone is set up in the fiber which satisfies the condition that the fiber section being heated is always cylindrical and is always heated uniformly. Allowing the hot zone length to change as taper elongation precedes any shape of the fiber taper can be generated. Three taper profiles namely linear (LP), parabolic (PP), and exponential linear

(EP) have been studied in literature for a fiber optic evanescent field absorption sensor as shown in Fig. 2 [22]. We consider these profiles for SPR based fiber optic tapered sensor. The different parts of the sensor are discussed below.

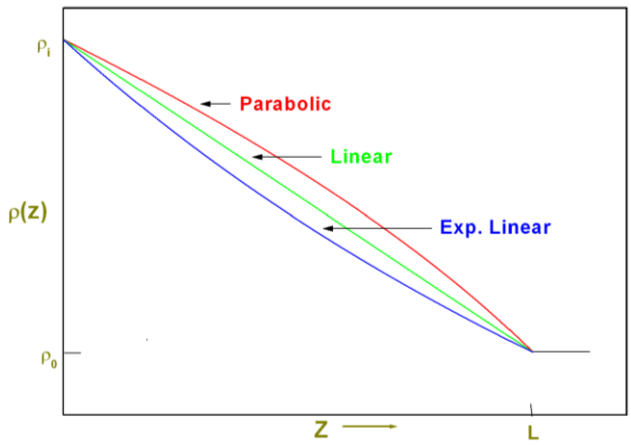

Figure 2: Three different taper profiles showing the linear, parabolic, and exponential-linear variation of core radius of taper with distance z from the input end of the taper.

A. *Core of the optical fiber*

For theoretical modeling, the optical fiber considered is a step-index multimode plastic clad silica fiber. Sinced the refractive index of the silica varies with the wavelength therefore the wavelength dependence of the refractive index (n1) of the silica core is given by Sellmeier dispersion relation:

$$n_1(\lambda)=\sqrt{1+\frac{a_1\lambda^2}{\lambda^2-b_1^2}+\frac{a_2\lambda^2}{\lambda^2-b_2^2}+\frac{a_3\lambda^2}{\lambda^2-b_3^2}} \quad (1)$$

a1, a2, a3, b1, b2, and b3 are the Sellmeier coefficients and λ is the wavelength of light used in μm. The values of these coefficients are given in the table below [25]:

a_1	0.6961663
a_2	0.4079426
a_3	0.8974794
b_1	0.0684043
b_2	0.1162414
b_3	9.896161

B. *Dispersion relation for plasmonic material*

For the wavelength dependence of the dielectric constant of the plasmonic material we have used the Drude model, given as

$$\varepsilon_m(\lambda)=\varepsilon_{mr}+i\varepsilon_{mi}=1-\frac{\lambda^2\lambda_c}{\lambda_p^2(\lambda_c+i\lambda)} \quad (2)$$

where λp and λc denote the plasma wavelength and collision wavelength, respectively. For gold, the following values of the plasma wavelength and collision wavelength are used: λ_P= 1.6826×10-7 M AND λ_C= 8.9342×10-6 M [26]

C. *Reflection Coefficient (R_p):*

We consider N-layer model to obtain the expression for amplitude reflection coefficient for p-polarized incident beam as shown in Fig. 3 [5].

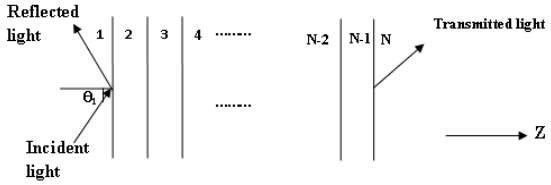

Figure 3: *N*-Layer model to determine the reflected light intensity.

In the present study, N is equal to 3. The layers are assumed to be stacked along the z-axis. The arbitrary medium layer is defined by thickness dk, dielectric constant εk, permeability μk, and refractive index nk. The tangential fields at the first boundary Z = Z1 = 0 are related to those at the final boundary Z = ZN-1 by

$$\begin{bmatrix}U_1\\V_1\end{bmatrix}=M\begin{bmatrix}U_{N-1}\\V_{N-1}\end{bmatrix} \quad (3)$$

In Eq. (3) U1 and V1 are the tangential components of electric and magnetic fields at the boundary of first layer, respectively; UN-1 and VN-1 are the corresponding fields at the boundary of Nth layer and M, known as characteristic matrix of the combined structure, is given by

$$M=\prod_{k=2}^{N-1}M_k=\begin{bmatrix}M_{11}&M_{12}\\M_{21}&M_{22}\end{bmatrix} \quad (4)$$

with

$$M_k=\begin{bmatrix}\cos\beta_k&(-i\sin\beta_k)/q_k\\-iq_k\sin\beta_k&\cos\beta_k\end{bmatrix} \quad (5)$$

where

$$q_k=\left(\frac{\mu_k}{\varepsilon_k}\right)^{1/2}\cos\theta_k=\frac{\left(\varepsilon_k-n_1^2\sin^2\theta_1\right)^{1/2}}{\varepsilon_k} \quad (6)$$

$$\beta_k=\frac{2\pi}{\lambda}n_k\cos\theta_k(z_k-z_{k-1})=\frac{2\pi d_k}{\lambda}\left(\varepsilon_k-n_1^2\sin^2\theta_1\right)^{1/2} \quad (7)$$

and θ_k is the angle of the ray normal to the kth interface. The amplitude reflection coefficient (r_p) for p-polarized incident wave is given by

$$r_p = \frac{(M_{11} + M_{12}q_N)q_1 - (M_{21} + M_{22}q_N)}{(M_{11} + M_{12}q_N)q_1 + (M_{21} + M_{22}q_N)} \quad (8)$$

Finally, reflectance (Rp) for p-polarized light is

$$R_p = |r_p|^2 \quad (9)$$

.

D. Reflected Power

The light is launched into the one end of the fiber through a broadband light source with proper optics. The other end is polished with silver paste to make it reflecting. The light rays that travels to the fiber gets reflected back due to this mirror end face. The end through which light is launched is connected with two way reflection probe. One end is used for light launching and other is used for collecting light back. This reflecting end is connected to a detection system to record the output signal. Consider the propagation of all the guided rays launched in the fiber using a collimated source and a microscope objective. The objective focuses the beam at the end-face of the fiber at axial point. The angular power distribution of rays guided in the fiber with θ as the angle of the ray with the normal to the core-cladding interface is given by [22]

$$dP \propto \frac{n_1^2 \sin\theta\cos\theta}{\left(1 - n_1^2\cos^2\theta\right)^2} d\theta \quad (10)$$

To determine the effective reflected power, the reflectance (Rp) for a single reflection is raised to the power of the twice the number of reflections the specific propagating angle undergoes with the sensor interface (Due to reflecting end each ray retraces its path). The guided rays in the uniform core fiber enter the sensing tapered region as shown in Fig. 1. Assuming adiabatic (slow) tapering, if ρ(z) is the taper radius at a distance z from the input end of the taper then the angle θ of the ray will transform into angle ϕ(z) in the tapered region and is given by [22]

$$\phi(z) = \cos^{-1}\left[\frac{\rho_i \cos\theta}{\rho(z)}\right] - \tan^{-1}\left(\frac{\rho_i - \rho_0}{L}\right) \quad (11)$$

In above equation, ρi and ρ0 are, respectively, the radii of the input (i.e. z = 0) and output end (i.e. z = L) of the taper. Further, the second term on right hand side is the taper angle (Ω) and L is the taper length. The taper radius varies with z in different fashion for different profiles given as [17]

Linear:

$$\rho(z) = \rho_i - \frac{z}{L}(\rho_i - \rho_0) \quad (12)$$

Exponential linear:

$$\rho_e(z) = (\rho_i - \rho_0)\left[e^{\left(-\frac{z}{L}\right)} - \frac{z}{L}\left(e^{-1}\right)\right] + \rho_0 \quad (13)$$

Parabolic:

$$\rho_P(z) = \left[\rho_i^{\,2} - \frac{z}{L}\left(\rho_i^{\,2} - \rho_0^{\,2}\right)\right]^{1/2} \quad (14)$$

If (θ1, θ2) is the range of incident angles of the rays launched at the input end of the taper, then at a distance z, this range alters to [ϕ1(z), ϕ2(z)] due to variation in core diameter in tapered region and the transmitted power at the output end of the fiber is given by

$$P_{trans} = \frac{\int_0^L dz \int_{\phi_1(z)}^{\phi_2(z)} R_P^{2N_{ref}(\theta,z)} \frac{n_1^{\,2}\sin\theta\cos\theta}{(1 - n_1^{\,2}\cos^2\theta)^2} d\theta}{\int_0^L dz \int_{\phi_1(z)}^{\phi_2(z)} \frac{n_1^{\,2}\sin\theta\cos\theta}{(1 - n_1^{\,2}\cos^2\theta)^2} d\theta} \quad (15)$$

The expressions for ϕ1(z) and ϕ2(z) can be found by substituting the value of θ in Eq. (11). For ϕ1(z), $\theta = \sin^{-1}(n_{cl}/n_1)$ and for ϕ2(z), $\theta = \pi/2$. Further, Nref is the number of reflections the ray of angle θ undergoes in the fiber with radius ρ(z) in the length L and is given as

$$N_{ref}(\theta, z) = \frac{L}{2\rho(z)\tan(\theta + \Omega)} \quad (16)$$

E. Sensitivity

In any fiber optic SPR sensor based on wavelength interrogation, the light from a polychromatic source is launched into one of the ends of the fiber and the spectrum of the transmitted light received at the other end is recorded to know the resonance wavelength (the wavelength corresponding to minimum transmission) corresponding to the refractive index of the sensing layer. If sensing region has a refractive index value of ns and εm is the dielectric constant of the metal layer in contact with sensing region, then the surface plasmon resonance occurs when the following condition is satisfied

$$\frac{2\pi}{\lambda} n_1 \sin\theta = \mathrm{Re}\left[\frac{2\pi}{\lambda}\left(\frac{\varepsilon_m n_s^2}{\varepsilon_m + n_s^2}\right)^{1/2}\right] \quad (17)$$

In Eq. (17), the expression on the left hand side is the propagation constant (Kinc) of the light incident at an angle θ while the right hand side represents the real part of surface

plasmon propagation constant (KSP). In the SPR sensor based on wavelength interrogation, Fixed angles of incidence are used and resonance wavelength (λres) is determined corresponding to refractive index of the sensing layer (ns). If the refractive index of the sensing layer is altered by δns, the resonance wavelength shifts by δλres. The sensitivity (Sn) of a SPR sensor with spectral interrogation is thus defined as [5]

$$S_n = \frac{\delta\lambda_{res}}{\delta n_s} \tag{18}$$

III.RESULTS AND DISCUSSIONS

Various important parameters used in the present study have been taken as: numerical Aperture of the fiber = 0.22, diameter of the fiber core (2ρi) = 600 μm, sensing region length (L) = 0.5 cm, gold layer thickness = 50 nm. In order to analyze the effect of taper ratio and taper profiles on the sensitivity, first of all we have to analyze the plasmonic resonance condition given by Eq. (17). As it is evident from Eq. (17), propagation constant (KSP) of surface plasmon wave (SPW) depends on the wavelength of the light as well as on the dielectric constant of metal layer (εm) and refractive index (ns) of sensing region. Whereas, the propagation constant (Kinc) of the incident wave depends on the angle and wavelength of the light ray as well as on the refractive index of the fiber core. Figure 4a depicts the variation of KSP1 (i.e. for ns1 = 1.333), KSP2 (for ns2 = 1.343) and Kinc with wavelength for the case when no tapering of the fiber probe is done. The angle of the ray is taken at the middle of the corresponding angle (ϕ1, ϕ2). As can be seen, KSP and Kinc curves cross each other at 613.86 nm for ns1 = 1.333 and at 648.46 nm for ns2 = 1.343. Thus, a shift (δλres) of 34.60 nm in resonance wavelength is observed for δns = 0.010. Now, the next task is to estimate the effect of taper profile (Eqs. 12-14) and taper ratio (ρi/ρo) on the shift (δλres) for the same value of δns. Figure 4b shows the variation of KSP1, KSP2, Kinc (LP), Kinc (PP) and Kinc (EP) with wavelength for taper ratio of 3.0. The curves corresponding to KSP1 and KSP2 are similar to those in Fig. 4a.

a.

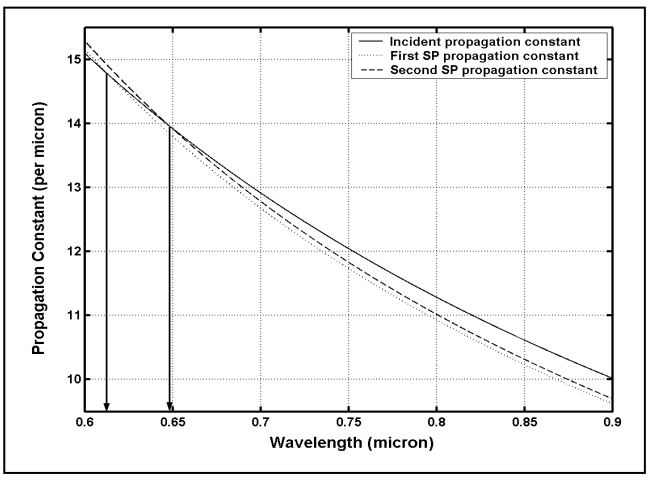

b.

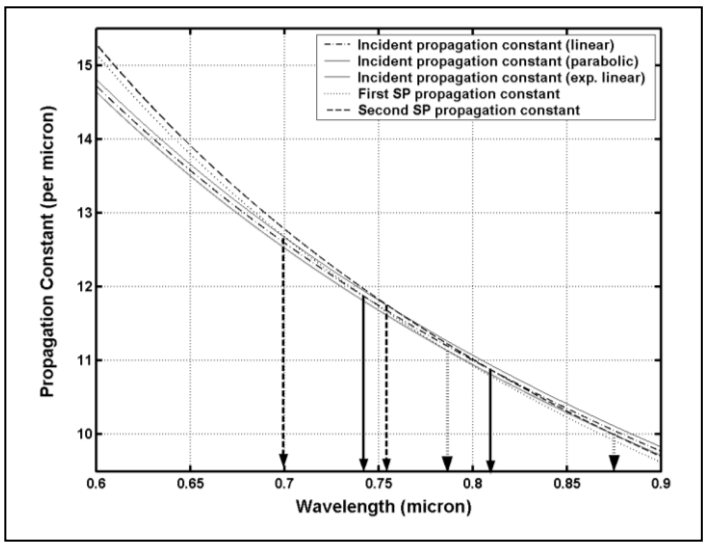

Figure 4: Variation of propagation constants for SPW and incident wave with wavelength for (a) Taper ratio = 1.0 and (b) Taper ratio = 3.0.

A noticeable change in Fig. 4b can be seen in terms of three-fold variation of Kinc corresponding to three different taper profiles. This happens due to two reasons: one, the angular range (ϕ1, ϕ2) is different for different taper profiles, and second, the dependence of both ϕ1 and ϕ2 on the taper ratio (Eq. 11). Consequently, the curves corresponding to KSP1 and KSP2 will intersect these three Kinc curves at six different points. In Fig. 4b, the above intersections corresponding to LP, PP, and EP have been shown with the help of two each solid, dashed, and dotted arrows, respectively. Table below shows the points of intersection and corresponding shift (δλres) for three taper profiles and three taper ratios.

Taper Ratio	Linear			Parabolic			Exp. Linear		
	λ_{r1} (nm)	λ_{r2} (nm)	$\Delta\lambda_r$ (nm)	λ_{r1} (nm)	λ_{r2} (nm)	$\Delta\lambda_r$ (nm)	λ_{r1} (nm)	λ_{r2} (nm)	$\Delta\lambda_r$ (nm)
1.0	613.86	648.46	34.60	613.86	648.46	34.60	613.86	648.46	34.60
2.0	684.09	735.56	51.47	671.24	719.23	47.99	699.57	755.48	55.91
3.0	741.94	811.59	69.65	699.65	755.58	55.93	787.58	875.08	87.50

It is quite visible from Fig. 4b and from Table above that for a given δns, maximum shift (i.e. δλres) is obtained for EP whereas minimum shift is found for PP. For LP, the corresponding shift is found to be in between the two. The similar trend was observed for all profiles at several angles in the corresponding range (ϕ1, ϕ2) and at several taper ratios between 1.0 and 2.2. This observation prepared the ground to check the present case when all the guided rays are launched together in the tapered fiber.

The calculations for transmitted power for a given refractive index of the sensing region, using Eq. (15), were

carried out with all the guided rays launched separately for all the three taper profiles with different taper ratios. From the plot of SPR spectrum resonance wavelength (λres) was determined. To appreciate the shift in resonance wavelength (i.e. δλres) due to the change in the refractive index (δns) much more precisely, the refractive index change (δns) was narrowed by taking the values of ns1 and ns2 as 1.333 and 1.335, respectively, (i.e., δns = 0.002). As was expected from above discussion, the shift (δλres) was found to be maximum for EP and minimum for PP with LP lying in between the two. The sensitivity of the sensor was calculated as defined by Eq. (18). Figure 5 gives the corresponding variation of the sensitivity (in μm per RIU) with taper ratio for all the three taper profiles. The figure shows that the sensitivity increases with an increase in taper ratio for any taper profile. Further, the sensitivity is maximum for exponential-linear profile (EP). The minimum sensitivity is observed for parabolic profile (PP). For the present set of design parameters mentioned above, a significant sensitivity enhancement of more than 80% in comparison to untapered fiber optic SPR sensor is observed at a taper ratio of 3.0 for exponential-linear taper profile (EP).

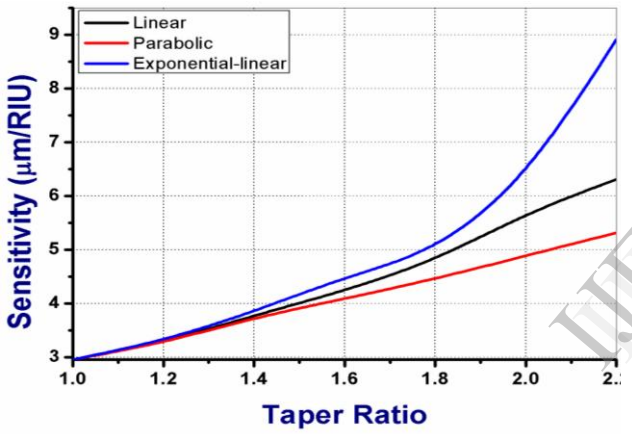

Figure 5: Variation of sensitivity (in μm per RIU) with taper ratio for three different taper profiles.

Apart from this explanation of the sensitivity enhancement with taper profile and taper ratio in terms of the shifting of resonance point (*i.e.*, $K_{SP} = K_{inc}$), another physically logical reason can be given in terms of evanescent wave absorption. By tapering the fiber we intend to broaden the angular range from (θ_1, θ_2) to (ϕ_1, ϕ_2), because lower value of angle means more spreading of the evanescent field into the region adjacent to fiber core. Hence the coupling between evanescent wave and SPW will become stronger and sensitivity is bound to increase due to tapering. Now, as far as the effect of taper profile is concerned, the angular range (ϕ_1, ϕ_2) in tapered region will be maximum for EP and minimum for PP according to Eqs. (13) and (14). This is why sensitivity is found to be maximum for EP. Furthermore, this improved coupling between evanescent wave and SPW due to tapered fiber causes SPR curve to broaden. However, the degree of SPR curve broadening is much lesser than the sensitivity enhancement with taper ratio and taper profile.

IV.CONCLUSIONS

In summary, a comprehensive theoretical model of an end face reflecting tapered fiber optic probe has been presented to evaluate the influence of tapering on the performance of a fiber optic SPR sensor. It is found from the study that the sensitivity of the sensor increases quite significantly with taper ratio. Also, the use of exponential-linear taper profile instead of linear or parabolic taper profile further improves the sensitivity. Therefore, high taper ratio with exponential-taper profile is recommended to design a highly sensitive fiber optic SPR probe. The light launching optics is also used for collecting the reflected light therefore it is more miniaturized as compared to other fiber optic probes.

REFERENCES

[1]. R. C. Jorgenson, S. S. Yee, "A fiber-optic chemical sensor based on surface plasmon resonance," Sens. Actuators B vol. 12 pp. 213 1993.
[2]. O. Esteban, R. Alonso, C. Navarrete, C. A. G. Cano, "Surface plasmon excitation in fiber-optic sensors: a novel theoretical approach" J. Lightwave Technol. Vol. 20 pp.448 2002.
[3]. L. K. Chau, Y. F. Lin, S. F. Cheng, T. J. Lin, "Fiber-optic chemical and biochemical probes based on localized surface plasmon resonance," Sens. Actuators B vol.113 pp.100 2006.
[4]. S. A. Zynio, A. V. Samoylov, E. R. Surovtseva, V. M. Mirsky, Y. M. Shirsov, "Bimetallic layers increase sensitivity of affinity sensors based on surface plasmon resonance," Sensors vol. 2 pp.62 2002.
[5]. A. K. Sharma, B. D. Gupta, "On the performance of different bimetallic combinations in surface plasmon resonance based fiber optic sensors,"J. App. Phys. vol. 101 093111 2007.
[6]. A.K. Sharma, B.D. Gupta, "Fiber optic sensor based on surface plasmon resonance with Ag-Au alloy nanoparticle films," Nanotechnology vol. 17 pp.124 2006.
[7]. G. G. Nenninger, P. Tobiska, J. Homola, S. S. Yee, "Long range surface plasmons for high resolution surface plasmon resonance sensors," Sens. Actuators B 74 pp. 145 2001.
[8]. Rajan, A. K. Sharma, B. D. Gupta, "Fiber optic sensor based on long range surface plasmon resonance," J. Opt.: Pure and App. Opt. vol.9 pp. 682 2007.
[9]. A. K. Sharma, Rajan, B. D. Gupta, "Influence of dopants on the performance of a fiber optic surface plasmon resonance sensor," Opt. Comm. vol.274 pp. 320 2007.
[10]. S. K. Misra and B. D. Gupta, " Surface plasmon resonance based fiber optic pH sensor utilizing Ag/ITO/Al/hydrogel layers," Analyst vol.138 pp. 2640 2013.
[11]. R. Tabassum, S. K. Misra and B. D. Gupta, "Surface plasmon resonance-based fiber optic hydrogen sulphide gas sensor utilizing Cu–ZnO thin films Physical Chemistry Chem. Phys. vol.15 11868 2013.
[12]. S. Singh, S. K. Misra and B. D. Gupta, "SPR based fibre optic biosensor for phenolic compounds using immobilization of tyrosinase in polyacrylamide gel," Sensors and Actuator B vol. 186 pp. 388 2013.
[13]. S. K. Misra, D. Kumari and B. D. Gupta, "Surface plasmon resonance based fiber optic ammonia gas sensor using ITO and polyaniline," Sensors and Actuator B vol. 171-172 pp. 976 2012.
[14]. Y.J. He, Y.L. Lo, J.F. Huang, "Optical fiber surface plasmon resonance sensor employing long period grating multiplexing," J. Opt. Soc. Am. B vol. 23 pp. 801 2006.
[15]. G. Nemova, R. Kashyap, ""Fiber Bragg grating assisted surface plasmon polariton sensor," Opt. Lett. vol.31 2118 2006.
[16]. X. Chen · R.-R.Wei · M. Shen · Z.-F. Zhang · C.-F. Li, "Bistable and negative lateral shifts of the reflected light beam from Kretschmann configuration with nonlinear left handed metamaterials," Applied Physics B vol.101 pp. 283 2010.
[17]. J. Villatoro, D. Monzon-Hernandez, E. Mejia, "Fabrication and modeling of uniform waist single mode tapered optical fiber sensor," App. Opt. vol. 42 pp. 2278 2003.

[18]. A. Diez, M. V. Andres, J. L. Cruz, "In line fiber optic sensors based on excitation of surface plasmon modes in metal-coated tapered fibers," Sens. Actuators B vol. 73 pp. 95 2001.
[19]. Y. C. Kim, W. Peng, S. Banerji, K. S. Booksh,"Fiber-optic surface plasmon resonance for vapor phase analyses," Opt. Letters vol 30 pp.2218 2005.
[20]. F.J. Bueno, O. Esteban, N.D. Herrera, M.C. Navarrete, A.G. Cano, "Sensing properties of asymmetric double layer covered tapered fibers," App. Opt. vol. 43 pp. 1615 2004.
[21]. B. Grunwald, G. Holst, "Fiber optic refractive index microsensor based on white light SPR excitation," Sens. Actuators A vol. 113 pp. 174 2004.
[22]. B. D. Gupta, C. D. Singh, "Fiber optic evanescent field absorption sensor: effect of launching condition and the geometry of the sensing region," Fiber and Integrated Optics vol.13 pp. 433 1994.
[23]. G. Chen, "Profile optimization of tapered waveguide sensors by fluorescence imaging," Proc. SPIE 5589 (2004) 70.
[24]. T.A. Birks, Y.W. Li, "The shape of fiber tapers," J. Lightwave Technol. Vol.10 pp. 432 1992.
[25]. A.K. Ghatak, K. Thyagarajan, " Introduction to Fiber Optics," Cambridge University Press, 1999, 85.
[26]. M.A. Ordal, L.L. Long, R.J. Bell, S. E. Bell, R.R. Bell, R.W. Alexander Jr., C.A. Ward, "Optical properties of the metals Al, Co, Cu, Au, Fe, Pb, Ni, Pd, Pt, Ag, Ti, and W in the infrared and far infrared," Appl. Opt. vol 11 pp.1099 1983.